Viscoelastic Characteristics of Magnetic Tapes with PEN Substrates

Brian L. Weick

Mechanical Engineering Department, School of Engineering and Computer Science, University of the Pacific, Stockton, California 95211

Received 25 May 2008; accepted 19 June 2008
DOI 10.1002/app.28932
Published online 17 October 2008 in Wiley InterScience (www.interscience.wiley.com).

ABSTRACT: Viscoelastic characteristics of magnetic tapes with poly(ethylene naphthalate) substrates were studied using experimental techniques. Measurements were made using samples cut from commercially available tapes, and solvents were used to remove front and/or back coat layers to obtain substrates and dual-layer samples. Experimental results allowed for fundamental compliance and viscosity parameters to be determined using a Kelvin-Voigt model. Rates of creep-compliance were also predicted, and comparisons were made with results for tapes that used poly(ethylene terephthalate) and aromatic poly(amide) substrates. Dynamic mechanical analysis (DMA) was used to help make correlations between viscous characteristics measured from the creep-compliance results and molecular characteristics of the substrates. Time-temperature superposition (TTS) was used to predict creep-compliance over extended time periods, and a rule-of-mixtures method was used to predict the compliance of constitutive layers. © 2008 Wiley Periodicals, Inc. J Appl Polym Sci 111: 899–916, 2009

Key words: creep; polyesters; viscoelastic properties; magnetic tapes; poly(ethylene naphthalate)

INTRODUCTION

Materials used to make digital magnetic tapes must be dimensionally stable to meet archival storage requirements. Users must be able to retrieve the information stored on these tapes, and typical specifications call for a 30+ year storage life. Since both temperature and humidity can affect the life of a tape, manufacturers recommend specific storage environments for their products. For example, a typical environment for the storage of tapes manufactured to the linear tape open (LTO) format is 16–32°C with a 20–80% relative humidity.[1] Because of these requirements, it is important to understand the properties and characteristics of the materials that comprise a magnetic tape through fundamental and applied research.

As an additional challenge, magnetic tape development needs to keep pace with challenges facing the storage industry as a whole. Competition with hard-disk drive manufacturers requires tape capacity to double approximately every two years, and tape manufacturers have developed roadmaps to meet this challenge.[2] Traditionally, manufacturers have made tapes and substrates thinner to increase the amount of tape that can be stored in a reel. Although this trend has continued, tape thickness is projected to decrease less over the next decade. However, other challenges must be met such as the increase in track density across the width of the tape measured as tracks-per-inch or TPI. As historical examples, 80 TPI was achieved in 1990 with the linear IBM 3490 tape, 256 TPI was achieved with the linear Quantum DLT 4000 tape in 1994, and LTO1 tapes had 923 TPI in 2000. Since that time, LTO2, LTO3, and LTO4 tapes have been released in 2002, 2004, and 2007 with TPIs of 1270, 1776, and 2228, respectively. Other linear tapes released in the 2004 to 2006 time frame include the Quantum SDLT-II and Sun/STK T10000 tapes used in this research. These tapes had increased TPIs of 1490 and 1870 when compared to their predecessors. Other tapes with high TPI values released in late 2005 and 2006 include the Quantum SDLT-S4 and IBM TS1120 with TPIs of 2988 and 2290, respectively. Lastly, helical tapes for data storage have achieved even higher TPI's such as Sony's AIT-1 tape in 1996 with a TPI of 2300, and the current SAIT-2 with a TPI of 5800.[2,3]

The increase in TPI is a challenge, because the 16 or 32 channel heads currently in use in linear drives must be able to read information from the tapes, which are comprised of viscoelastic materials that undergo complex stress states when they are stored in a reel and used in a drive.[4,5] This causes the tape to stretch, and expand or contract circumferentially, tangentially, and radially when it is stored in the reel. Such dimensional instabilities can render the

Correspondence to: B. L. Weick (bweick@pacific.edu).

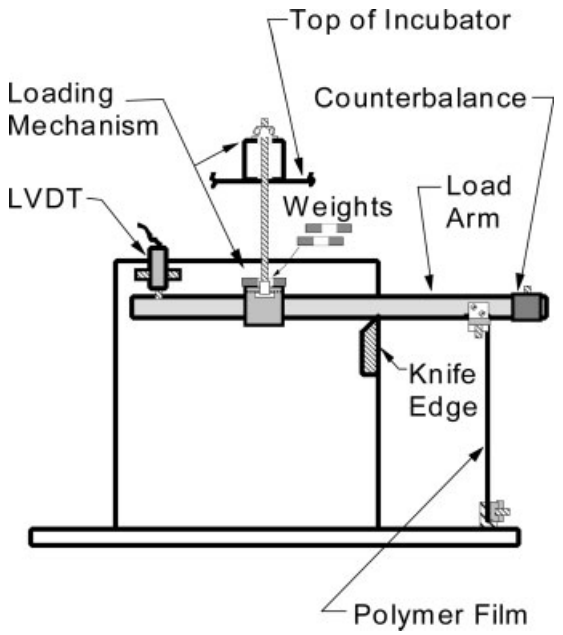

Figure 1 Schematic view of a creep tester for evaluating the creep behavior of magnetic tape materials.

tape unreadable after archival storage. Measuring and predicting these instabilities is a challenge due to the complexities of the tape itself, which can be considered to be a multilayer composite consisting of a front coat (magnetic + nonmagnetic layer), substrate, and back coat. Each of these layers contributes to the viscoelastic characteristics and associated dimensional instabilities of the tape.

As outlined in the experimental procedure, well-established methods were used in this study to determine the viscoelastic characteristics for magnetic particle (MP) tapes that use a poly(ethylene naphthalate) or PEN substrate. To assist with archival life predictions, experiments were not only performed using the MP-PEN tapes, but additional experiments were also performed with the substrates used for these tapes as well as specially prepared dual-layer samples. Part of this procedure included determining the fundamental compliance and viscosity parameters using results from custom creep-compliance experiments. These parameters describe the viscoelastic characteristics of the tape materials, and can be used in models to predict behavior of the tape when it is stored in a reel.[6–8] In addition, the parameters can be used to predict the rate of creep-compliance.[9] Time-temperature superposition (TTS) together with a rule-of-mixtures method can also be used to predict creep-compliance over extended time periods for the constitutive layers of the tape as well as the tape itself.[7,8] Comparisons will be made with an MP tape that uses a poly(ethylene terephthalate) or PET substrate, and a tape with a metal-evaporated (ME) magnetic layer that uses an aromatic poly(amide) or Aramid substrate. Results from dynamic mechanical analysis (DMA) of the MP-PEN tapes will help determine relationships between the viscoelastic characteristics of the substrate materials and their molecular characteristics.

Experimental and analytical procedure

Creep experiments were performed with a custom-built apparatus housed in a temperature-controlled incubator. A schematic of this test apparatus is shown in Figure 1. Humidity was controlled by using desiccant in the test chamber at low temperatures (30°C); at high temperatures (50 and 70°C) the chamber dries-out and the humidity was less than 1%. Test samples that were typically 330–400 mm long were evaluated. The samples had 200 mm long test sections, and were 12.7-mm wide. Environmental conditions were monitored using a hygrometer and temperature sensor, and the test apparatus utilized linear variable differential transformers (LVDT's) connected to a LabView-based 16-bit A/D system to measure extension or contraction of the samples. The experiments were performed at a 7.0 MPa stress level that corresponds with typical drive tensions.

An outline of the experimental procedure and analytical techniques used to acquire and process data from the custom creep apparatus is described in Table I. Other articles by Weick[8] and Weick and Bhushan[6–8] provide a thorough description of these techniques, and will only be described briefly and expanded-upon as necessary in this article.

TABLE I
Outline of Experimental and Analytical Procedure

Perform creep-compliance experiments at 30, 50, and 70°C for 50 to 100+ h. At least three repeats are performed at each temperature level
Use four different types of samples: (1) Tape, (2) Front coat and substrate, (3) Substrate and back coat, and (4) Substrate only. Layers are removed using methyl ethyl ketone (MEK)
Calculate time-dependent creep-compliance $D(t)$ and initial creep-compliance D_o from repeat experiments at each temperature level
Curve fit data to the Kelvin-Voigt viscoelastic model using a Levenburg-Marquardt algorithm to determine and analyze viscoelastic properties
Use time-temperature superposition to predict creep-compliance for extended time periods (>100 years) at a reference temperature of 30°C
Use a rule-of-mixtures approach to predict creep-compliance for the front and back coats
Predict rate of creep-compliance using curve fit parameters. This rate of creep-compliance can be referred to as creep velocity
Compare results with known properties and characteristics of the constitutive tape materials to gain a more fundamental understanding of the dimensional stability of the materials

TABLE II
Magnetic Tape Specifications

	LTO2	LTO3	T10000	MP-PET	ME-Aramid
Tape manufacturer and trade name	IBM TotalStorage Ultrium Data Cartridge		Sun/STK T10000 Tape Cartridge	Quantum Super DLTtape II Media	Sony AIT-3 Tape Cartridge
Native capacity (GB)	200	400	500	300	100
Compressed capacity (GB)	400	800	1000	600	260
Substrate material	PEN: poly(ethylene naphthalate)			PET: poly(ethylene terephthalate)	Aramid: aromatic polyamide
Magnetic layer	MP: magnetic particle				ME: metal-evaporated
Tape width (mm)	12.65				8.0
Track density (tracks-per-Inch, TPI)	1270	1776	1870	1490	4600
Track pitch (μm)	20.0	14.3	13.6	17.1	5.5
Track pitch divided by tape width (μm/m)	1595	1130	1074	1348	690
Nominal tape thickness (μm)	8.9	8.0	6.5	8.0	5.3
Measured tape thickness (μm)	8.46	7.87	6.55	–	–
Measured substrate thickness (μm)	6.12	6.04	5.13	–	4.5 (nominal)
Meas. front coat and substrate thick (μm)	8.13	7.37	6.15	–	–
Meas. substrate and back coat thick (μm)	6.58	6.48	5.54	–	–
Calculated front coat thickness (μm)	2.01	1.33	1.02	–	–
Calculated back coat thickness (μm)	0.46	0.44	0.41	–	–

Thickness measurements made with a Mahr gage accurate to ±25.4 nm.

Table II provides specifications for the magnetic tapes used in this study. The primary focus was on MP tapes with PEN substrates, which are referred to as MP-PEN tapes. Therefore, the properties and characteristics of LTO2, LTO3, and T10000 MP-PEN tapes were evaluated, and these tapes reflect the increasing storage capacity trend from 2002 to 2006 as well as the increase in TPI. In addition, these MP tapes decreased in thickness from 8.9 μm for LTO2, to 8.0 μm for LTO3, and 6.5 μm for T10000. Furthermore, the PEN substrates used for these three tapes decreased in thickness from 6.12 to 6.04, and 5.13 μm, respectively. Front coat and back coat thicknesses also decreased as shown in Table II. Specifications and thicknesses are also included for a Quantum SDLT-II tape made with a PET substrate as well as a Sony AIT-3 tape made with an Aramid substrate. The Quantum tape has an MP coating and will be referred to as an MP-PET tape. The Sony tape has an ME coating and will be referred to as an ME-Aramid tape. Experiments performed with these tapes have been discussed by Weick,[7] and will be used to make comparisons with the MP-PEN tapes (LTO2, LTO3, and T10000) that are the focus of the study.

Viscoelastic analysis method

As outlined in Table I, creep-compliance experiments were performed at elevated temperatures using samples of magnetic tape materials. Using output from the LVDT's, the creep strain, $\varepsilon(t)$, can be determined as well as the creep-compliance, $D(t)$, as the initial steps in the viscoelastic analysis.

$$\varepsilon(t) = \frac{\Delta l(t)}{l_o} \tag{1}$$

$$D(t) = \frac{\varepsilon(t)}{\sigma_o} = \frac{\Delta l(t)}{\sigma_o l_o} \tag{2}$$

$\Delta l(t)$ is the change in length of the test specimen as a function of time, l_o is the original length of the test specimen, $\varepsilon(t)$ is the amount of strain the film is subjected to, σ_o is the constant applied stress, and $D(t)$ is the tensile creep-compliance of the test specimen as a function of time.

Creep-compliance data for the test specimens are modeled using a generalized Kelvin-Voigt viscoelastic model, which has the following mathematical form:

$$D(t) = D_o + \sum_{k=1}^{K} D_k[1 - \exp(-t/\tau_k)] \tag{3}$$

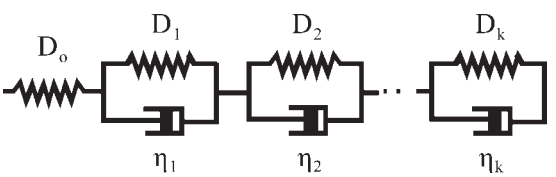

Figure 2 The Kelvin-Voigt model used to express the elastic and viscous characteristics of polymeric materials.

where, D_o is the instantaneous compliance at time $t = 0$, D_k is the discrete compliance term, and t_k is the discrete retardation time for each Kelvin-Voigt element.

Equation (3) is typically represented as a series of parallel springs and dashpots connected to a single spring. This mechanical analog is shown in Figure 2, and is indicative of a viscoelastic polymer which has an amorphous phase with mainly unoriented molecules, and a crystalline phase which contains oriented molecules. Components of the polymeric structure which respond instantly to an applied stress are modeled as a single spring with an instantaneous compliance D_o. Components of the polymeric structure which do not respond instantly but are deformed in a time-dependent manner are modeled as multiple elements consisting of springs and dashpots acting in parallel. Each element contains a spring which has a compliance D_k, and a dashpot with a viscosity equal to η_k. The retardation time for each k^{th} element is defined below:

$$\tau_k = \eta_k D_k \tag{4}$$

Experimental data sets are fitted to eq. (3) using a nonlinear least-squares technique known as the Levenberg-Marquardt method.[10] This method is used to find the best-fit parameters τ_k and D_k for a Kelvin-Voigt model with multiple elements. Previous work by Weick and Bhushan[6,7] to determine the viscoelastic characteristics of alternative polymeric substrates used for magnetic tapes showed that two to three elements are typically required for a reasonable fit.

Figure 3 shows examples of how two-term and three-term curve fits can be applied to LTO3 tape data. Raw data from the 50°C experiments are shown in gray, and variation in the data is due to the ±0.1°C temperature cycling in the chamber. Both the two-term and three-term curve fits are shown. Figure 3 shows the raw data and curve fits on linear and log scales. For time periods less than 10 h, the two-term and three-term curve fits work equally as well. Note the similarity between the compliance, retardation time, and viscosity terms for the first two Kelvin-Voigt elements. However, the three-term model is a better fit for the data during the 10–100 h time period as shown in Figure 3. Note that the first and second sets of viscoelastic parameters (D_1, τ_1, D_2, τ_2) are all positive. This makes the derived viscosity terms (η_1, η_2) positive. In comparison, D_3 is negative and τ_3 is positive for the third set of parameters, which makes η_3 negative. The difference in signs can be attributed to the decrease in creep-compliance after ~ 10 h. Characteristics of the substrate appear to control this behavior, and will be discussed along with viscoelastic parameters at other temperatures for the three MP-PEN tapes studied.

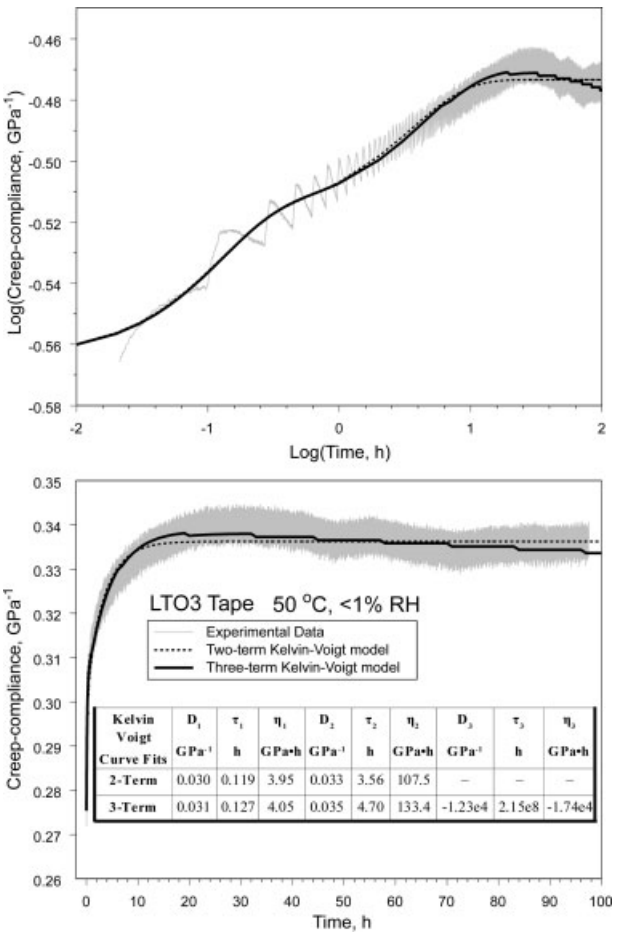

Kelvin Voigt Curve Fits	D_1 GPa^{-1}	τ_1 h	η_1 GPa•h	D_2 GPa^{-1}	τ_2 h	η_2 GPa•h	D_3 GPa^{-1}	τ_3 h	η_3 GPa•h
2-Term	0.030	0.119	3.95	0.033	3.56	107.5	–	–	–
3-Term	0.031	0.127	4.05	0.035	4.70	133.4	-1.23e4	2.15e8	-1.74e4

Figure 3 Example of curve fit using a two-term versus a three-term Kelvin-Voigt model.

The rate of creep-compliance or "creep velocity" is indicated by the slope of the creep-compliance curve. Using the first derivative of the Kelvin-Voigt model and the curve fit parameters D_k and τ_k, the creep velocity can be calculated for each tape sample as a function of time.

$$\frac{dD(t)}{dt} = \sum_{k=1}^{K} \frac{D_k}{\tau_k} \exp(-t/\tau_k) \tag{5}$$

where $dD(t)/dt$ is the creep velocity in GPa^{-1}/h.

TTS has been used in past research to predict long-term creep behavior at ambient temperature.[7–9,11] This analytical technique utilizes creep measurements at elevated temperature levels to predict behavior at longer time periods. In this research, data sets acquired at 30, 50, and 70°C are superimposed at a reference temperature of 30°C to determine long-term creep behavior over an extended time period. The rationale for this methodology stems from the observation that most polymers will behave in the same compliant manner at a particular high temperature as they will when they are deformed at a particular

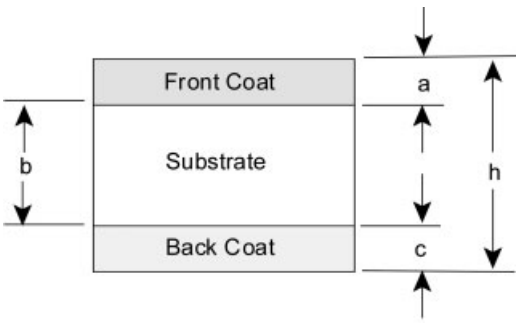

Subscripts

a, b, c — front coat, substrate, back coat

t — tape

ab — combined front coat and substrate

bc — combined substrate and back coat

Figure 4 Nomenclature used to describe tape layers.

slow rate at room temperature. This means that there is a correspondence between time (or rate of deformation) and temperature.

By performing experiments with specially prepared dual layer samples, a rule of mixtures method can be used to determine viscoelastic properties of the front coat (magnetic and nonmagnetic layer), substrate, and back coat.[6–8] The procedure calls for the magnetic tape to be modeled as a multiple layer polymer composite laminate as shown in Figure 4.

Using the equation shown below, the creep-compliance of the front coat can be determined if data are available from creep-compliance experiments performed using a front coat substrate material and the substrate only. See Figure 4 for nomenclature.

$$D_a(t) = \left[\left(\frac{a+b}{a}\right)\left(\frac{1}{D_{ab}(t)}\right) - \left(\frac{b}{a}\right)\left(\frac{1}{D_b(t)}\right)\right]^{-1} \quad (6a)$$

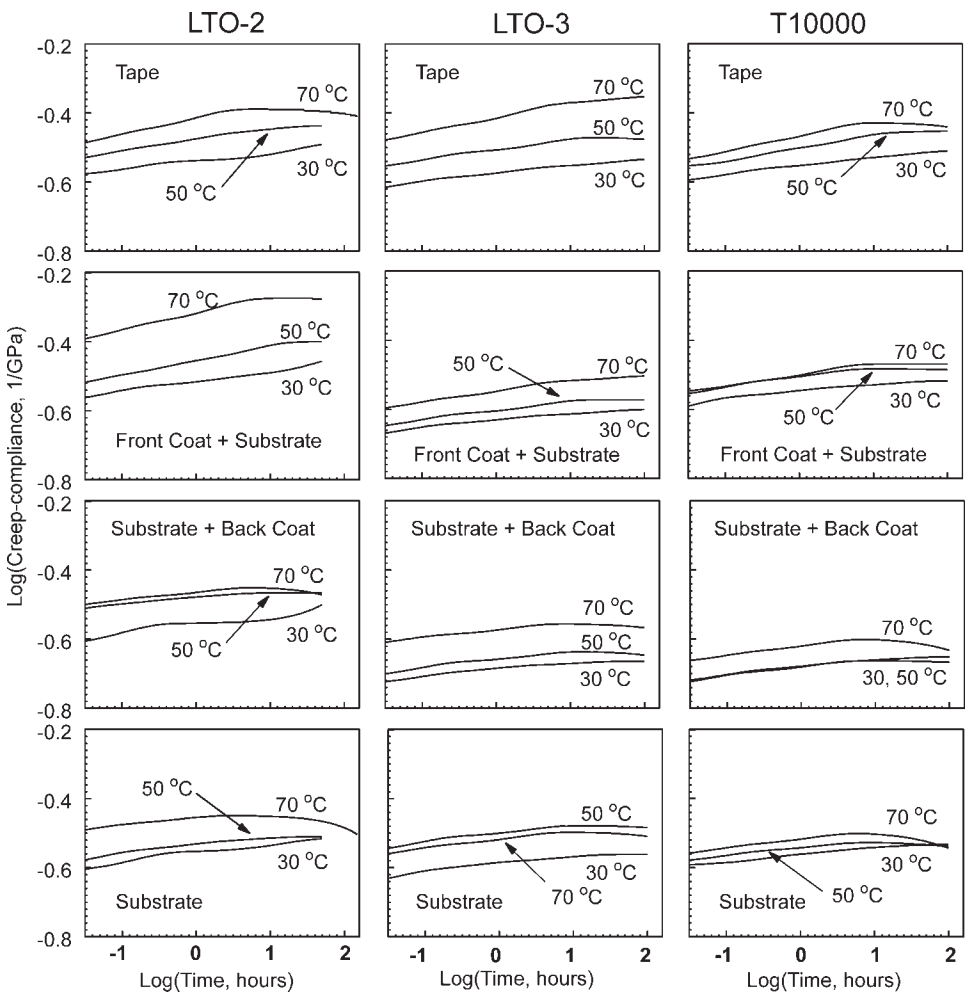

Figure 5 Creep-compliance curves for MP-PEN tapes, substrates, and dual-layer front coat substrate and back coat substrate samples. Curve fits are shown after fitting the data sets to the Kelvin-Voigt model.

TABLE III
Average Initial Creep-Compliance Values (D_o) and Standard Deviations Calculated Using Three Repeat Experiments

		Log(Initial Creep-Compliance (D_o), 1/GPa)					
		LTO-2		LTO-3		T10000	
		Average	Std. Dev.	Average	Std. Dev.	Average	Std. Dev.
30°C	Tape	−0.575	0.070	−0.631	0.016	−0.604	0.061
	FC + Subs	−0.566	–	−0.685	0.014	−0.594	0.070
	Subs + BC	−0.561	–	−0.735	0.029	−0.730	0.033
	Substrate	−0.606	0.032	−0.657	0.059	−0.626	0.079
50°C	Tape	−0.549	0.037	−0.564	0.027	−0.560	0.047
	FC + Subs	−0.548	–	−0.659	0.009	−0.556	0.065
	Subs + BC	−0.535	–	−0.715	0.018	−0.742	0.006
	Substrate	−0.598	0.011	−0.561	0.056	−0.587	0.028
70°C	Tape	−0.512	0.075	−0.495	0.016	−0.547	0.030
	FC + Subs	−0.412	–	−0.610	0.041	−0.568	0.023
	Subs + BC	−0.511	–	−0.621	0.016	−0.674	0.009
	Substrate	−0.505	0.005	−0.575	0.014	−0.569	0.020

Average initial values calculated 20 s after start of loading period.

Similarly, the creep-compliance of the back coat can be determined if data are available from creep-compliance experiments performed using a substrate + back coat material and the substrate only.

$$D_c(t) = \left[\left(\frac{b+c}{c}\right)\left(\frac{1}{D_{bc}(t)}\right) - \left(\frac{b}{c}\right)\left(\frac{1}{D_b(t)}\right)\right]^{-1} \quad (6b)$$

Once the creep-compliances of the front coat and back coat have been determined using eqs. (6a) and (6b), the creep-compliance for a complete tape can be predicted using eq. (6c).

$$D_t(t) = \left[\frac{1}{h}\left(\frac{a}{D_a(t)} + \frac{b}{D_b(t)} + \frac{c}{D_c(t)}\right)\right]^{-1} \quad (6c)$$

Data sets determined using eq. (6c) for a complete tape utilize creep-compliance data for the front coat, substrate, and back coat from three separate experiments. To verify this technique, the data sets determined using eq. (6c) can be compared with actual measured data sets for a magnetic tape.

RESULTS AND DISCUSSION

Creep-compliance characteristics for PEN-based tapes

Results from experiments performed at 30, 50, and 70°C are shown in Figure 5. These results are for three types of MP-PEN tapes including LTO-2, LTO-3, and T10000 tapes. Four types of samples were prepared for each tape at each temperature: (1) tape as-cut from the cartridge, (2) front coat substrate with the back coat removed, (3) substrate back coat with the front coat removed, and (4) substrate with front and back coat removed. Initial creep-compliances, D_o, are listed in Table III for the experiments shown in Figure 5. Note that standard deviations are included for LTO-3 and T10000, because repeat experiments were performed at each temperature for these tape samples. Only D_o values are included for LTO-2, and these results are from past work described by Weick[8]. The methodology and rationale for determining the average initial creep-compliances is also described by Weick[8] along with a thorough description of the results for the LTO-2 samples. As expected, higher temperatures lead to higher average creep-compliances, which is shown in Figure 5 and Table III.

The trend lines shown in Figure 5 represent curve fits using the Kelvin-Voigt model, eq. (3). As described previously, six parameters are typically needed for the curve fits including D_1, τ_1, D_2, τ_2, D_3, and τ_3. The viscosity terms (η_1, η_2, and η_3) are derived quantities as shown in eq. (4). Figures 6 and 7 are plots of the compliance and viscosity terms for LTO3 and T10000 samples as a function of the temperature levels at which the experiments were performed. (Curve fits for the LTO2 samples were performed, but are inconclusive because of the lack of repeat experiments performed for these samples.[8]) Compliance terms shown in Figure 6 correspond with the springs in the Kelvin-Voigt model, and indicate how the samples respond to the applied stress in a manner that stores and releases energy in a recoverable manner. The viscosity terms shown in Figure 7 correspond with the dashpots in the Kelvin-Voigt model, and indicate how the samples respond to the applied stress in a manner that dissipates energy in a nonrecoverable manner.

From Figure 6, as the temperature increases, the first two compliance terms D_1 and D_2 tend to increase for the samples, although there does appear

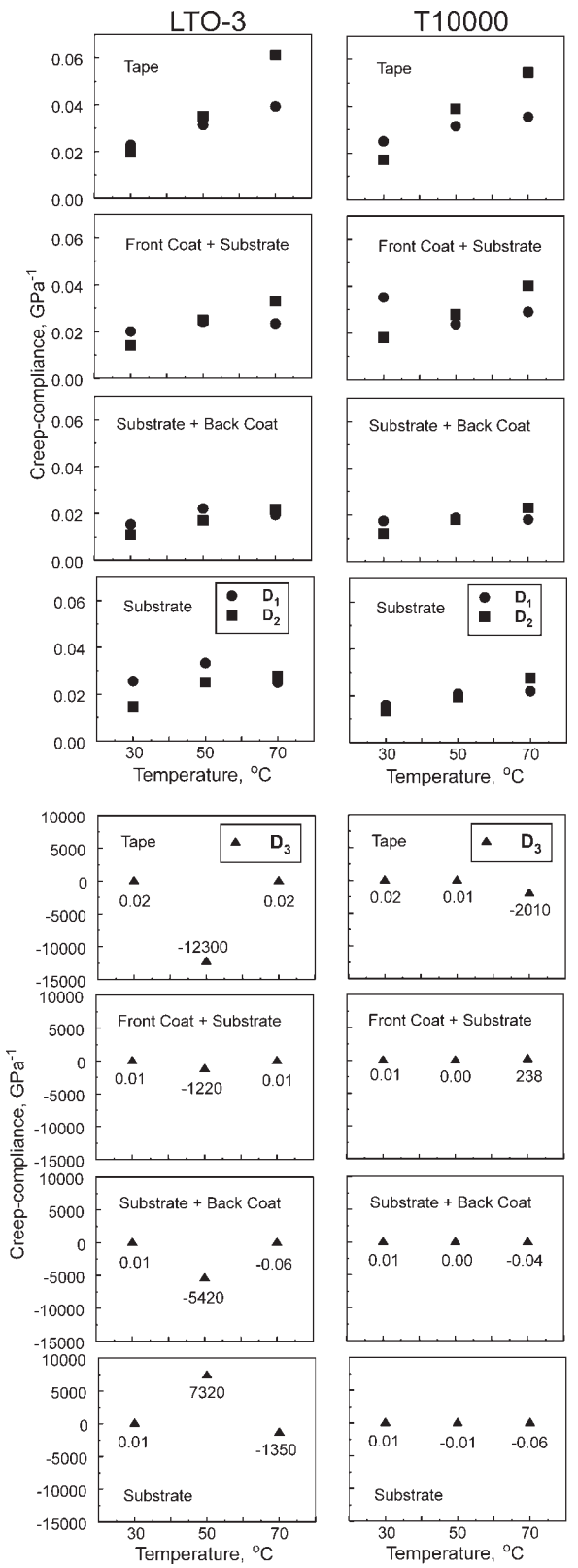

Figure 6 Creep-compliance terms, D_1, D_2, and D_3, for MP-PEN (LTO-3 and T10000) tape samples.

to be a decrease in D_1 for the LTO3 substrate back coat and substrate samples. Furthermore, D_2 tends to be higher than D_1 for the tape and front coat substrate samples at the 50 and 70°C temperatures, whereas D_2 tends to be lower or similar to D_1 for the substrate back coat and substrate samples at

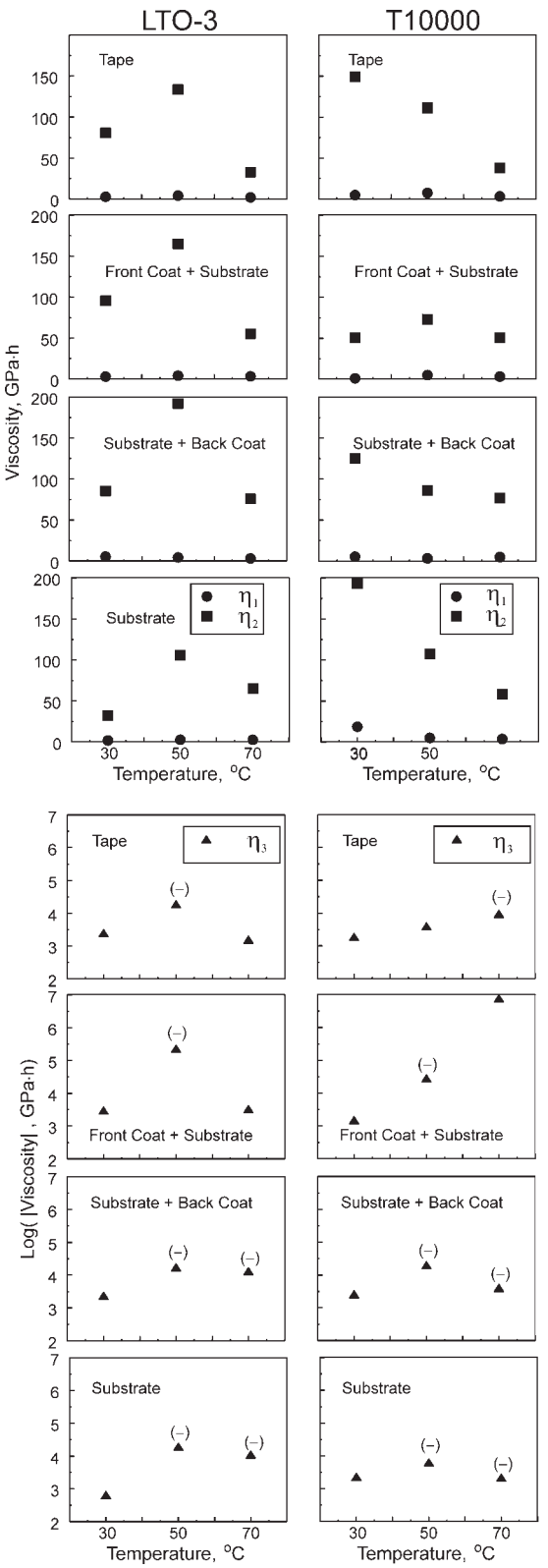

Figure 7 Viscosity terms, η_1, η_2, and η_3 for MP-PEN (LTO-3 and T10000) tape samples.

30°C. This indicates that the increasing compliance of the elastomeric binder for the front coat at elevated temperatures could play more of a role in recoverable dimensional changes in the tape. The D_3 terms shown in the separate graphs in Figure 6 are more difficult to interpret. A highly positive D_3 compliance term is present at 50°C for the LTO3 substrate sample, whereas highly negative D_3 compliance terms are present at 50°C for the LTO3 tape and dual-layer samples. D_3 results for the T10000 samples appear to be less variable. From Figures 3 and 5, the D_3 compliance terms correspond with the peaks and roll-off observed in the creep-compliance data at 50 and 70°C after 10 h. Note that the retardation times, τ_k, are functions of the compliance and viscosity terms, D_k and η_k as shown in eq. (4). Therefore, high values of either D_k or η_k in the Kelvin-Voigt model can cause the exponential terms, $\exp(-t/\tau_k)$, to tend to be 1, which makes $[1 - \exp(-t/\tau_k)]$ close to zero. This appears to be the case for the third term of the Kelvin-Voigt model, with high values of D_3 or η_3 playing a subtle role in determining the shape of the creep-compliance curves during the longer time periods.

As shown in Figure 7, the initial viscosity terms, η_1, are negligible regardless of temperature. This supports the notion that the tape responds initially in a recoverable, compliant manner. (Note that the initial compliance terms, D_1, in Figure 6 are low, but not negligible compared to the other compliance terms.) However, the second viscosity terms, η_2, are significantly higher. For LTO3, peak values of η_2 occur at 50°C when compared to the 30 and 70°C values. For T10000, the η_2 values tend to decrease with an increase in temperature, although the front coat and substrate sample appears to reach a peak at 50°C. For LTO3 the samples are behaving in a more viscous manner at 50°C, and T10000 samples are generally behaving in a more viscous manner at 30°C. This corresponds with more energy dissipation and nonrecoverable deformation. For LTO3, since all the samples include the substrate, and the substrate behaves in a manner that is similar to the other samples, it is reasonable to state that the 50°C peak in η_2 is related to substrate behavior. Note that all the η_3 values are high on a negative or positive scale, which is why logs of the absolute values of the η_3 values are plotted in Figure 7. As was observed for the η_2 terms, peaks in the third viscosity terms, η_3, are also observed at 50°C for LTO3, although these terms are negative as indicated by the (–) sign underneath the data points in the semi-log plots. T10000 samples also tend to show these relative peaks at 50°C for substrate and back coat and substrate samples, but the front coat appears to play a role in causing the relative increase in viscosity at 70°C. For both LTO3 and T10000, the tape and front coat substrate samples show similar trends for η_3 values, and the η_3 values for the substrate back coat trends are similar to those for the substrate. However, as was stated for the compliance terms, high viscosity values also cause the $[1 - \exp(-t/\tau_k)]$ term to be close to zero, and the affect of the third term of the Kelvin Voigt model can only be seen in the log scale plots at longer time periods as shown in Figure 3.

Creep velocity of PEN-based tapes

Although some information about the rate of creep-compliance (creep velocity) can be gathered through visual examination of the curves shown in Figure 5, it is more informative to graph the creep velocity as demonstrated in Figure 8 for LTO-3 samples at 50°C. Three D_k and three τ_k values from the curve fit of the creep-compliance data were used in the first derivative of the Kelvin-Voigt equation, eq. (5), to generate the creep velocity curves shown in Figure 8. The upper graph of Figure 8 shows a stepwise decrease in the creep velocity out to 15 to 25 h for the four LTO3 samples. This stepwise decrease is because of the use of the multiple curve fit values.

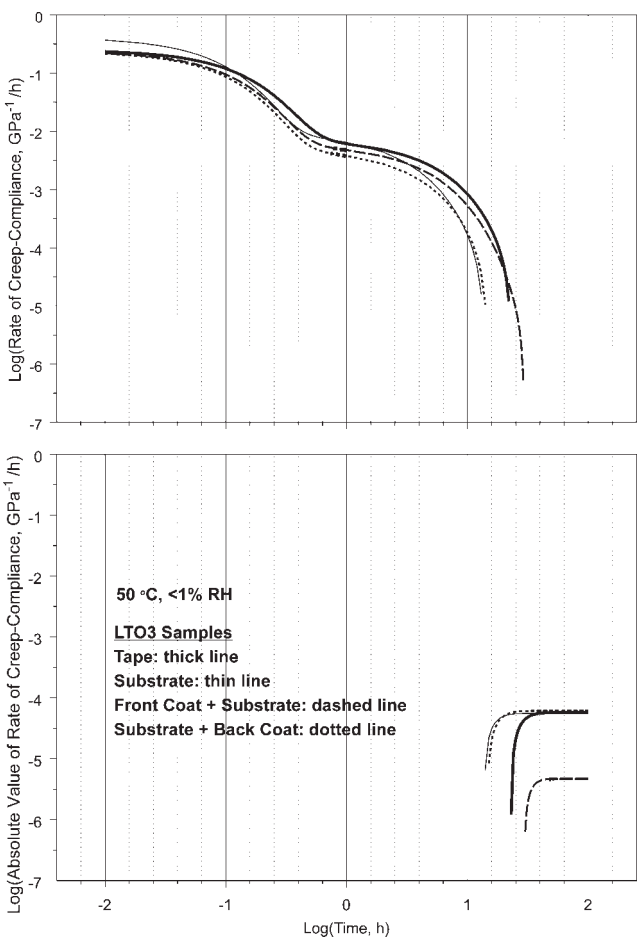

Figure 8 Rate of creep-compliance for LTO-3 samples.

Since a log scale was used to plot the data, only positive rates of creep-compliance could be plotted out to the 15–25 h time periods. Past these time periods, the slope of the creep-compliance curves is negative. As a result, absolute values of the creep velocities were determined, which allowed the final time periods to be plotted in the lower graph of Figure 8.

The decreasing trend to the creep velocity for PEN substrates has been noted in past research,[9] and this appears to be reflected in the rates for the tape and dual-layer samples shown in Figure 8. However, it is interesting to note that the rates of creep-compliance for the tape and front coat substrate follow a similar trend, which shows that the compliance characteristics of the front coat play an important role in determining the creep-compliance of the tape in addition to the role of the substrate. The rates of creep-compliance for the substrate and substrate back coat samples also follow a similar trend, which shows the role of the substrate in determining the creep-compliance of the substrate back coat sample.

A closer examination of Figure 8 can provide more information about the viscoelastic characteristics of the tape and its constitutive layers. Initially, the rate of creep-compliance for the substrate is higher than the rates for the other samples, and this trend continues for the first 0.1 h, with lower rates for the tape, front coat substrate, and substrate back coat, respectively. After $\sim$ 0.1 h, the rate of compliance for the tape tends to equal or exceed that of the substrate. After $\sim$ 4 h the tape and front coat substrate samples appear to always have higher rates of creep-compliance than the substrate and substrate back coat samples.

When the creep velocity goes through the reversal from positive to negative during the final time periods, there appears to be a rapid decrease in creep velocity after which a steady-state creep velocity is reached as shown by the horizontal lines in Figure 8 for time periods greater than 25 h. Similar characteristics were observed for all types of MP-PEN samples at 50 and 70°C during the final time periods, which indicate that the PEN substrate characteristics play an important role.

It is informative to compare creep velocities for all the MP-PEN tapes evaluated in this study and also compare them with creep velocities determined for MP-PET and ME-Aramid samples evaluated in past research. As shown in Figure 9, all MP-PEN tapes (LTO-2, LTO-3, and T10000) show similar decreasing trends at 50°C. Creep velocities in later time periods do show some possible differences between the three MP-PEN tapes, although these appear to be related to the times at which the lowest creep velocities are reached. Note that LTO-3 shows the creep-velocity reversal from a positive to negative slope, which was not observed at time periods less than 100 h for

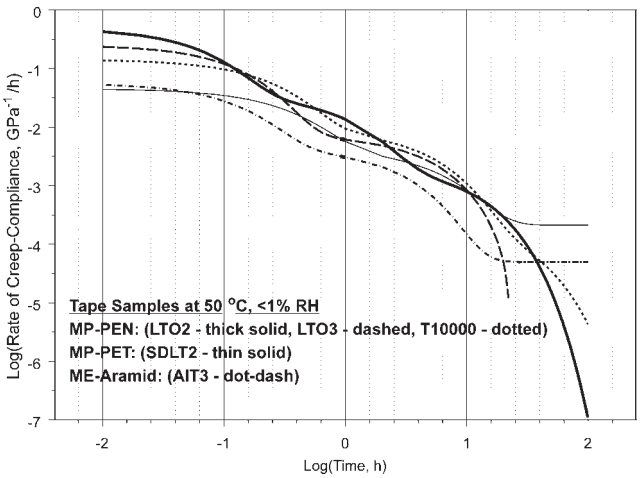

Figure 9 Rate of creep-compliance for MP-PEN tapes compared with compliance rates for MP-PET and ME-Aramid tapes.

the other MP-PEN samples at 50°C. However, these creep-velocity reversals are prevalent at 70°C.

The MP-PET and ME-Aramid tapes show lower overall creep velocities during the initial time periods when compared to the MP-PEN tapes. The MP-PET tape behaves in a manner that is similar to the MP-PEN tapes during the middle of the time period shown in Figure 9. After a log time of $\sim$ 1.4 (25 h), the MP-PET tape appears to reach a steady-state creep-velocity. The ME-Aramid experiences the same type of behavior, and also reaches a steady-state creep velocity after a log time of $\sim$ 1.2 (16 h). Note that the ME-Aramid tape also shows a lower overall creep-velocity than the MP-PET tape after a log time of -1 (0.1 h). In comparison, the MP-PEN tapes show a decreasing trend to their creep velocities that continues to decrease after a log time of 1 (10 h). Similar results were discussed in past research by Weick and Bhushan[9] for experiments performed with PEN, PET, and ME-Aramid substrate samples cut from wide-stock film.

Figure 10 shows creep velocity results for all the MP-PEN samples at 30, 50, and 70°C. Results are shown for the tape, front coat substrate, substrate back coat, and substrate samples cut from LTO-2, LTO-3, and T10000 tapes. The graphs show an overall similarity between the creep velocities, and only an overlay at specific temperatures as shown in Figure 8 reveals the similarity between tape and front coat substrate creep velocities as well as the similarity between the substrate and substrate back coat creep velocities. Furthermore, there is a general tendency for the lowest creep velocities to be reached after longer time periods for 30°C when compared to 50°C and 70°C. The substrate behavior appears to govern the similarity between the different types of samples since it is the common element

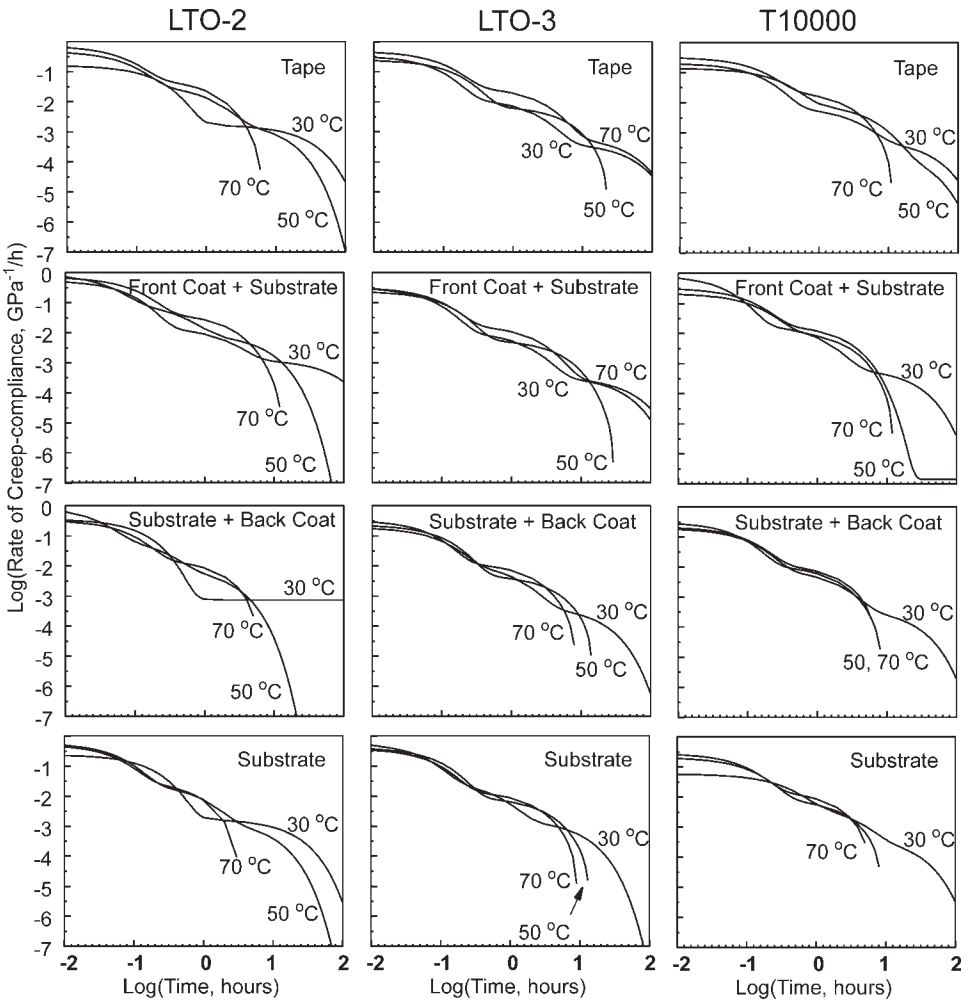

Figure 10 Rate of creep-compliance for MP-PEN tape samples at 30, 50, and 70°C.

in all samples. Note that the reversal in creep-velocity depicted in Figure 8 from positive to negative was typically observed at 70°C, and to a lesser extent at 50°C.

DMA of PEN substrates

To help understand the viscoelastic behavior of the PEN substrates used for the LTO-3 and T10000 tapes, an experimental technique known as DMA was utilized. This technique is sometimes referred to as Dynamic Mechanical Thermal Analysis, and subjects small samples of thin polymer films to dynamic stress–strain conditions in a temperature-controlled test apparatus.[12] When the polymer film samples are subjected to a sinusoidal strain, $\varepsilon(t)$, the sinusoidal stress, $\sigma(t)$, measured on the sample reaches peak values at slightly later time periods. This is depicted in Figure 11, and the time lag, Δt, is due to the specific viscoelastic characteristics of the polymer film being tested. As shown in eq. (7), a corresponding phase angle shift can be calculated using the frequency of the sinusoidal strain used for the experiment.

$$\delta = (2\pi f)\Delta t \tag{7}$$

where, δ is the phase angle shift, f is the test frequency, and Δt is the time lag between the strain and stress. Using this information, the storage modulus, E', loss modulus, E'', complex modulus, E^*, and loss tangent, $\tan(\delta)$ can be calculated using eqs. (8a–d).

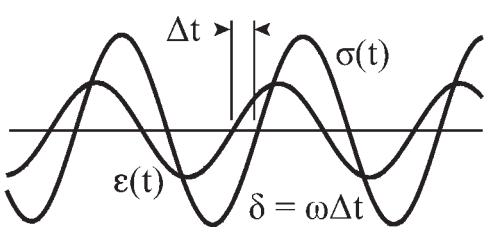

Figure 11 Schematic drawing of sinusoidal strain and stress signals from dynamic mechanical analysis.

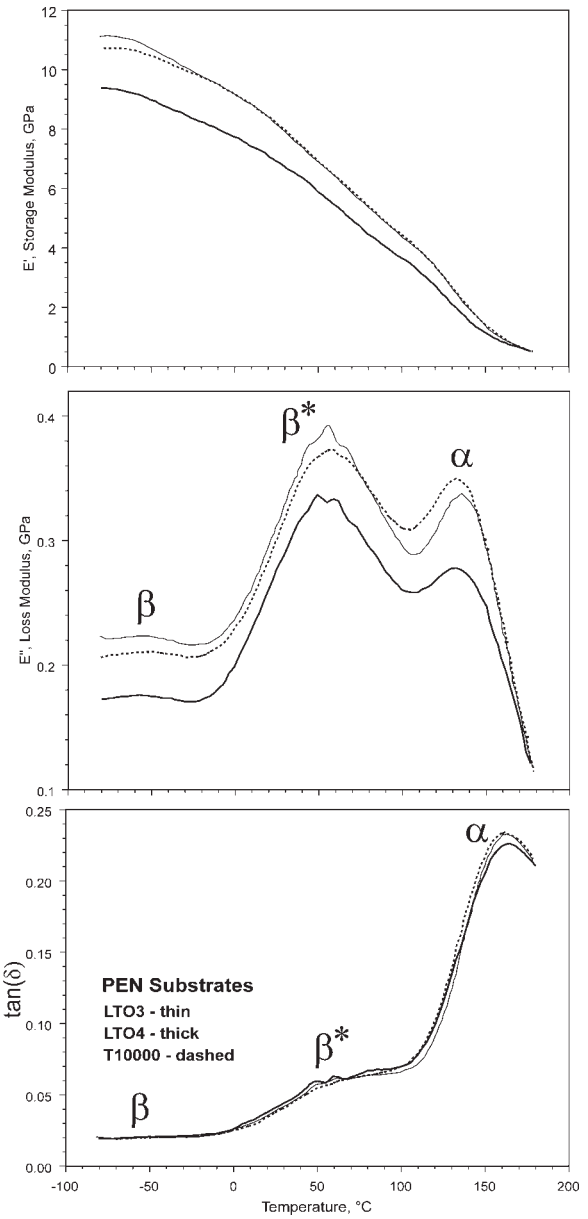

Figure 12 Dynamic mechanical analysis results for three MP-PEN tapes (LTO-3, T10000, and LTO-4).

$$E' = \cos(\delta)\left[\frac{\sigma}{\varepsilon}\right] \tag{8a}$$

$$E'' = \sin(\delta)\left[\frac{\sigma}{\varepsilon}\right] \tag{8b}$$

$$|E^*| = \sqrt{(E')^2 + (E'')^2} \tag{8c}$$

$$\tan(\delta) = \frac{E''}{E'} \tag{8d}$$

The storage (or elastic) modulus, E', is a measure of the component of the complex modulus, E^*, which is in-phase with the applied strain, and the loss (or viscous) modulus, E'', is a measure of the component which is out-of-phase with the applied strain. The in-phase stress and strain results in elastically stored energy that is completely recoverable, whereas out-of-phase stress and strain results in the dissipation of energy that is nonrecoverable and lost to the system. The loss tangent, tan(δ), is simply the ratio of the loss (or viscous) modulus to the storage (or elastic) modulus.[12]

Figure 12 shows storage modulus, loss modulus, and loss tangent results for the PEN substrates used for LTO-3, T10000, and LTO-4 tapes. (Note that the creep experiments were performed for LTO-2, LTO-3, and T10000, but these experiments could not be performed for LTO-4 in time for inclusion in this publication due to the extended period of time it takes to perform the creep experiments. However, it was felt that DMA results for LTO-4 could be performed in time for this publication, and should be included to lend insight into the dimensional stability of this recent generation of LTO tape.) In general, the storage modulus shown in Figure 12 is high at low temperatures, and decreases in a nonlinear manner as temperature increases. This decrease in the elastic character of the substrates corresponds with the general increase in compliance with temperature shown in Figure 5. From Figure 12, the loss modulus for the PEN substrates is initially low at temperatures below 0°C, but increases above this temperature and reaches the β* peak at approximately 50°C. (The asterisk is used to distinguish the β* peak at ~50°C from the β peak that occurs at approximately −70°C.[13]) After reaching the β* peak, the loss modulus decreases to a relative minimum, and then increases to another peak labeled α at 130°C before decreasing significantly at higher temperatures. The β* peak is attenuated and the α peak is amplified when the loss tangent is calculated using the ratio of the loss and storage moduli. Furthermore, the peaks are shifted to the right with the α peak appearing to shift more than the β* peak. The loss tangent α peak occurs at ~ 160°C, and is a measure of the glass transition. Above this temperature, long-range motion of the polymer chains occurs in the glassy regions of the PEN substrates.

Because the loss modulus corresponds with the viscous character of the substrate, it is interesting to note that at 50°C, the β* peak in Figure 12 corresponds with the peak in the η_2 viscosity term at 50°C determined from LTO3 creep experiments as shown in Figure 7. Recall that the D_2 and η_2 terms describe the intermediate range for the creep-compliance behavior, whereas D_1 and η_1 describe the initial behavior, and D_3 and η_3 describe the behavior at longer time periods. η_1 terms are small relative to the η_2 terms, and the large magnitude of the D_3 and η_3 terms render the $[1 - \exp(-t/\tau_k)]$ term in the Kelvin-Voigt model to be small. However, the relative peaks in the η_3 terms for the substrate and

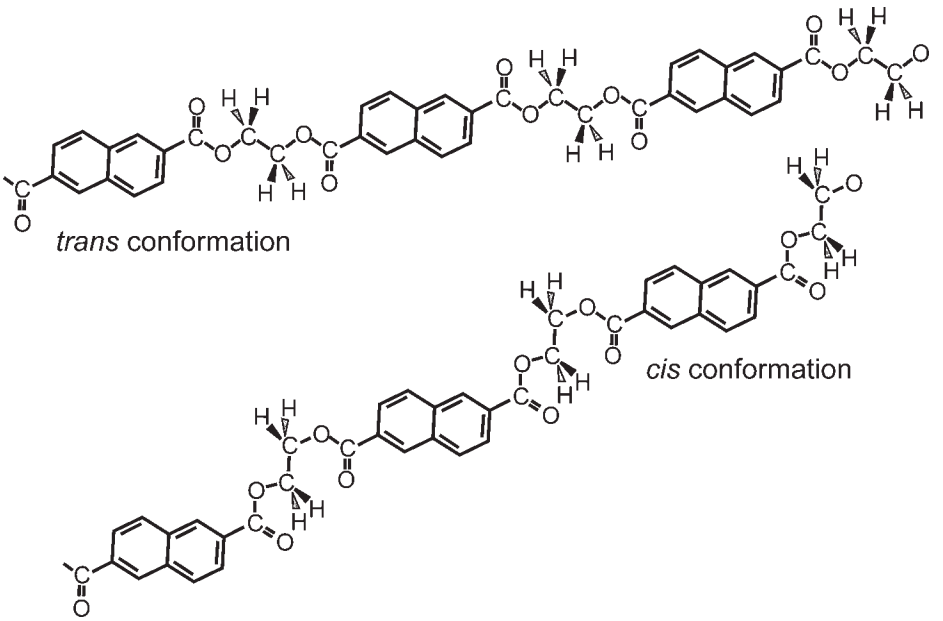

Figure 13 Schematic drawing of PEN macromolecules showing *cis* and *trans* conformations.

substrate back coat samples also lends support to the relationship between the wide β* peak at 50°C.

The β* peak in the DMA loss modulus at 50°C and associated peak in the η_2 viscosity from the creep experiments at 50°C indicate that there is an increase in energy dissipation and nonrecoverable deformation of the PEN polymer, although it should be understood that the DMA experiments were performed at 10 Hz with a controlled strain amplitude, whereas the creep experiments utilized the application of a constant stress resulting in a time-dependent creep strain. The 50°C temperature is an upper design temperature for magnetic tapes, and even when stored at lower temperatures, the behavior observed at 50°C can occur after longer time periods due to the viscoelastic characteristics of the PEN polymer. As a result, it is important to gain some insight into this behavior at 50°C, since a more thorough understanding would help with the design of future PEN-based tapes, which would require enhanced dimensional stability due to the need for increases in track density referred to in the Introduction.

Canadas et al.[13] have noted that the β* peak is not present in PET, which suggests that the presence of this peak in the PEN DMA loss modulus is probably due to the relative motion of the two naphthalene rings present in the polymer chain. Jeong et al.[14] also measured the β* relaxation in PEN and attributed this relaxation to out-of-plane motion of the naphthalene rings or their aggregates, and Higashioji and Bhushan[11] have noted this mechanism as a major contributor to creep behavior of PEN film in the −20 to 80°C range. They also noted that Gillmor and Green[15] suggested an interlayer slippage mechanism for the naphthalene rings. A thorough study of the dynamic behavior of PEN versus PET has been presented by Tonelli,[16] who noted the importance of the geometries of the ester groups attached to the naphthalene rings in PEN. He described the conformations of PEN versus PET, and noted that the rotation of the naphthalene structure in PEN sweeps through a larger volume during rotation. Because of interaction with other polymer chains, this makes PEN less flexible than PET.[16] When these concepts are combined with the simple observation that the β* peak is present in PEN and not in PET, this leads to the motion of the naphthalene rings and attached molecular groups in PEN as the likely cause of the energy dissipation and nonrecoverable deformation at 50°C. However, as noted in a recent study by Hakme et al.,[17] the β* relaxation is more complex than this and can be related to naphthalene aggregate motions as well as plastic deformation of the PEN film and the presence of a stable fibrillar crystalline morphology together with a structurally relaxed amorphous phase. In addition, Hakme et al.[17] quantitatively measured a rigid amorphous fraction that could also play a role in the viscoelastic behavior of PEN, and he conjectured that there is a directional nature to the viscoelastic behavior related to intrafibrillar versus interfibrillar amorphous phases.

A closer examination of the loss modulus β* peaks in Figure 12 reveals the presence of sharper peaks on shoulders within the wider peaks for LTO3 and T10000, as well as double peaks within the β* peak for LTO4. Canadas et al.[13] observed double peaks in

the loss modulus measured at 1 Hz, and attributed these peaks to the *trans* and *cis* conformations for PEN. Tonelli[16] also referred to these conformations in his discussion of the rotation of the naphthalene rings and attached ester groups. As shown in Figure 13, the *trans* conformation for PEN leads to increased crystallinity due to alignment of the naphthalene rings, whereas the *cis* conformation leads to an increase in amorphous characteristics due to misalignment of the rings.

The relationship between the *trans* conformation and crystallinity, and *gauche* conformation and amorphous regions was observed by Berg and Wei,[18] and they used infrared spectroscopy to determine the presence of these conformations as a method for determining the amount of crystalline and amorphous regions in PET. Note that the *gauche* conformation referred to by Berg and Wei[18] for PET is similar to the *cis* conformation for PEN, and using specific IUPAC nomenclature both conformations could be referred to as +synclinal.[19] Berg and Wei[18] also noted the importance of the proportion of amorphous and crystalline regions on achieving the extreme dimensional stability of biaxially oriented PET needed for adhesive tape to support arrays of parallel optical fibers. They indicated that the amorphous region is important for dimensional stability, and should not be too small.

The dual nature of the β* peaks in Figure 12 and attribution to the *trans* and *cis* conformations suggests the important of amorphous and crystalline regions for the dimensional stability of PEN films. LTO3 and T10000 have the sharper peaks corresponding with the *trans* conformation and more crystalline regions, whereas LTO4 has dual peaks associated with both *trans* and *cis* conformations. Therefore, LTO4 is likely to have a higher proportion of amorphous regions because of the presence of the *cis* conformation. Furthermore, these amorphous regions could take on the characteristics of the rigid amorphous discussed by Hakme et al.,[17] and this could make the PEN substrate more dimensionally stable as predicted by Berg and Wei.[18] From Figure 12, this is supported by the lower overall loss modulus for LTO4 in addition to the lower overall storage modulus when compared to LTO3 and T10000.

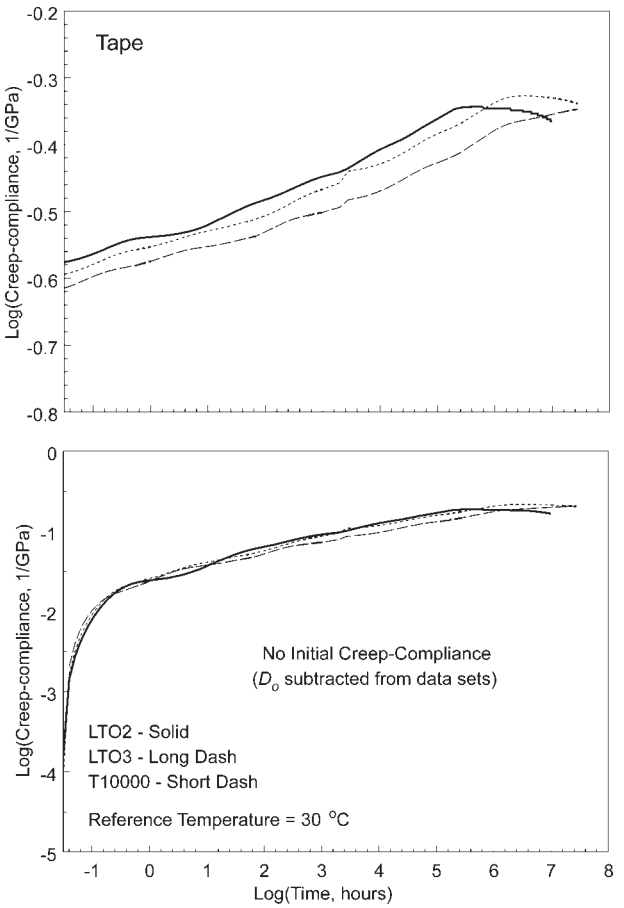

Figure 14 Time-temperature superposition for MP-PEN tapes.

TTS (PEN-based tapes and dual-Layer samples)

Magnetic tapes and substrates

Using the creep-compliance results shown in Figure 5 at 30, 50, and 70°C, the TTS process can be used to predict creep-compliance at a reference temperature of 30°C over an extended time period of $\sim 10^7$ h. These predictions are shown in Figure 14 for the three types of MP-PEN tapes. Note that the slopes of the lines are similar out to $\sim 10^5$ hours, which is indicative of the similar creep velocities. However, the initial compliance values, D_o, are slightly different although this difference could be attributed to variations during the initial loading of the tapes as shown by the standard deviations in Table III. The peaks in creep-compliance followed by decreases at 70°C can be observed in the upper graph of Figure 14 for LTO2 and T10000 after 10^5 h, with a less prevalent change-in-slope observed for LTO3. These peaks can be attributed to the β* transitions experienced by the substrates rather than transitions in the front coat or back coat of the samples.

Since the initial creep-compliance, D_o, can be considered to be due to the elastic response, these values have been subtracted-out in the lower graph of Figure 14. This results in similar creep-compliance curves for all three types of MP-PEN tapes. The initial viscoelastic response out to 1 h is similar followed by a long-term response that is similar out to 10^5 h. Because of the increase in the log creep-compliance scale, the peaks observed after 10^5 h are less prevalent when the D_o terms are subtracted-out.

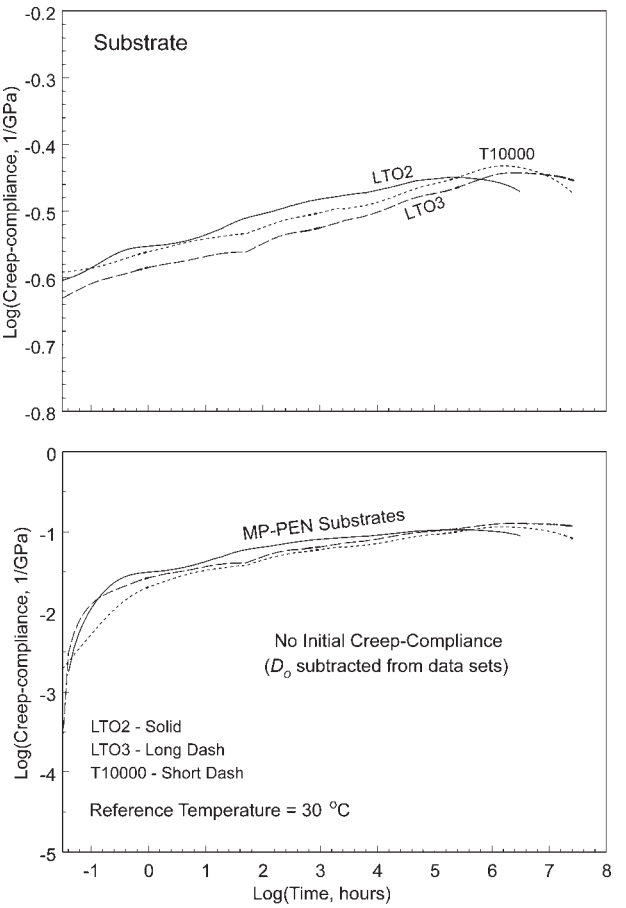

Figure 15 Time-temperature superposition for MP-PEN substrates.

The overall creep-compliance is lower for the PEN substrates shown in Figure 15 when compared to the MP-PEN tapes shown in Figure 14. However, as was observed for the tapes, the PEN substrates have similar creep-compliance characteristics, which is particularly noticeable when the initial compliance, D_o, is subtracted-out from the data sets. Furthermore, the roll-off in the substrate curves are similar to what was observed for the tape indicating that this behavior is due to the substrate and not due to other tape layers.

Dual-layer samples

Differences in creep-compliance are observable when the front coat substrate results from the TTS process are viewed in Figure 16, which once again shows the data sets with and without the initial compliance, D_o. There is more of a separation due to the initial elastic compliance, and the LTO2 front coat substrate sample appears to creep at a faster rate as shown by the slope of the lines in Figure 16. If D_o is subtracted-out, the initial viscoelastic response of the three MP-PEN front coat substrate samples appears to be similar during the first 0.1 h (log time of −1). However, after this initial viscoelastic response, the LTO2 sample not only experiences a higher overall creep-compliance, it also creeps at a slightly faster rate than LTO3 and T10000. Note a slight change-in-slope still occurs at longer time periods due to the substrate, but this is less prevalent because of the influence of the front coat. Differences in creep-compliance between the LTO2, LTO3, and T10000 front coat substrate samples could be due to the increase in magnetic particle density, which could inhibit the movement of the elastomeric binder typically used for MP-PEN tapes.

Long-term creep-compliance characteristics of the substrate back coat samples are shown in Figure 17 after the TTS process. When the initial creep-compliance, D_o, is included in the upper graph of Figure 17, there appears to be a large offset between LTO2 when compared to LTO3 and T10000. This offset is less significant when the D_o values are subtracted from the data in the lower graph of Figure 17, and could be due to errors in the initial loading of the LTO2 samples, which were only tested once at each temperature. Characteristics of the substrate are apparent in the substrate back coat data shown in Figure 17, since the curves are similar to what is

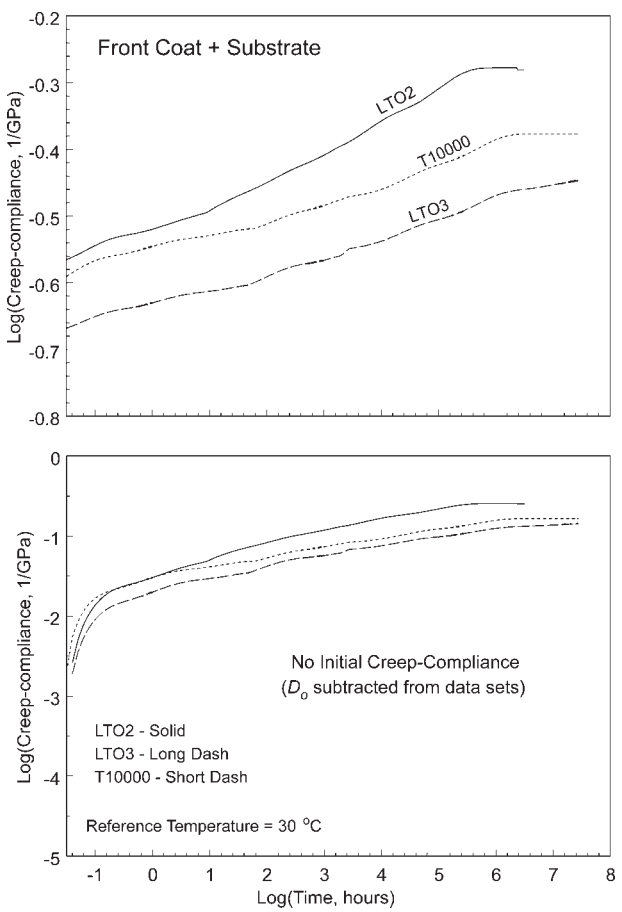

Figure 16 Time-temperature superposition for MP-PEN front coat substrate samples.

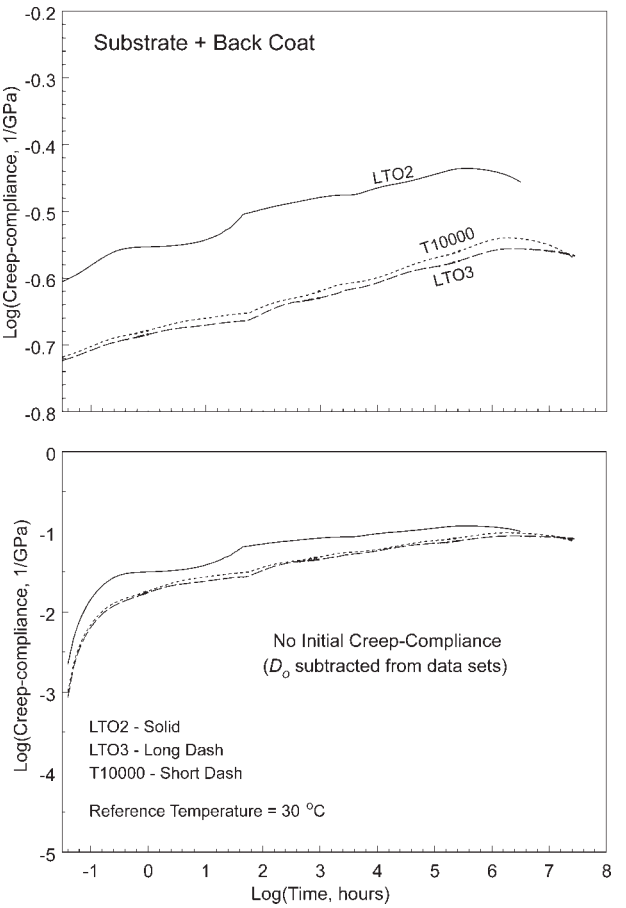

Figure 17 Time-temperature superposition for MP-PEN back coat substrate samples.

shown in Figure 15 for the substrates. As a result, the back coat for the MP-PEN tapes is not regarded as having a significant effect on the creep characteristics of the magnetic tape as whole.

Front coat and back coat creep characteristics

Using the rule-of-mixtures method described by eqs. (6a) and (6b),[6–8,20] the creep characteristics of the front coat can be separated-out as shown in Figure 18. D_o has been subtracted from the data in the lower graph. Similarly, the creep characteristics of the back coat can be separated-out as shown in Figure 19.

Figure 18 shows that there is clearly a difference between the front coat creep-compliance characteristics for LTO2, LTO3, and T10000. The higher overall creep-compliance for the LTO2 tape is clear in Figure 18 as well as the increase in creep after a shorter period of time. Creep-compliances for T10000 and LTO3 are lower than LTO2, and the increase in creep is more gradual and occurs after a longer time period for LTO3 when compared to T10000 or LTO2. When D_o is subtracted-out, this trend is also present and the sudden increases in creep-compliances are more pronounced at longer time periods for LTO2 and T10000 when compared to LTO 3. Note that the sharp dip in the LTO2 curve is likely due to similar creep-compliances for the front coat substrate and the substrate data at this time period. Since the inverse of the front coat substrate data is subtracted from the inverse of the substrate data in the rule-of-mixtures calculation, it is particularly sensitive to time periods where the data sets are similar.[6–8]

Back coat creep-compliance characteristics in Figure 19 show that T10000 and LTO3 have similar characteristics, whereas the back coat for LTO2 has a higher overall creep-compliance. Note that there is a lot of variation in the LTO2 back coat data, which has been attributed to the similarity between the substrate back coat creep-compliance data and the substrate data.[6–8] When D_o is subtracted-out in Figure 19, the back coat compliance for T10000 and LTO3 follow the same trend with the back-coat compliance higher for T10000. Although the back coat compliance for LTO2 is still higher when D_o is subtracted-out, a large discontinuity can be observed at $\sim$ 10 h, which could once again be attributed to the sensitivity of the rule-of-mixtures calculation to

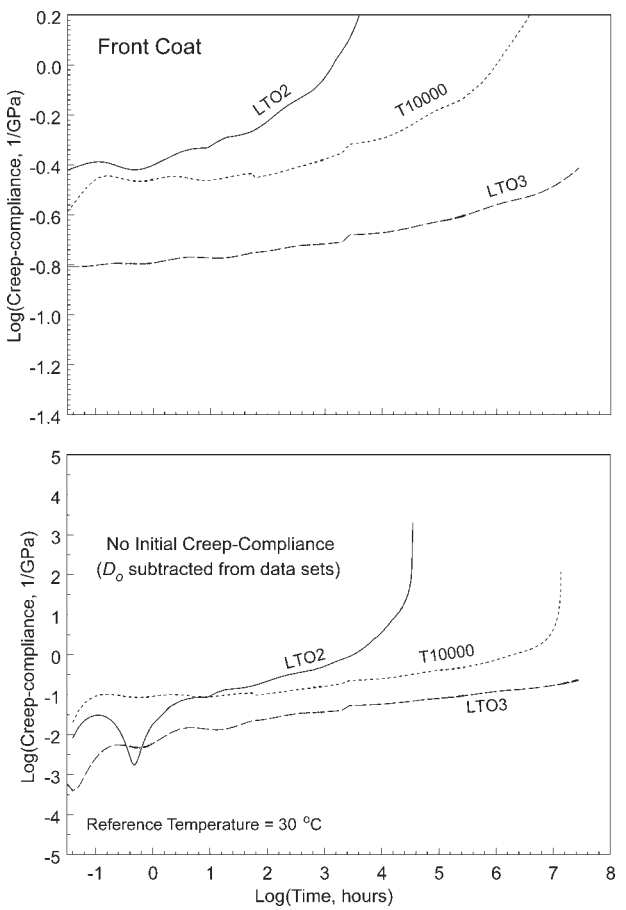

Figure 18 Time-temperature superposition for MP-PEN front coat samples from rule-of-mixtures analysis.

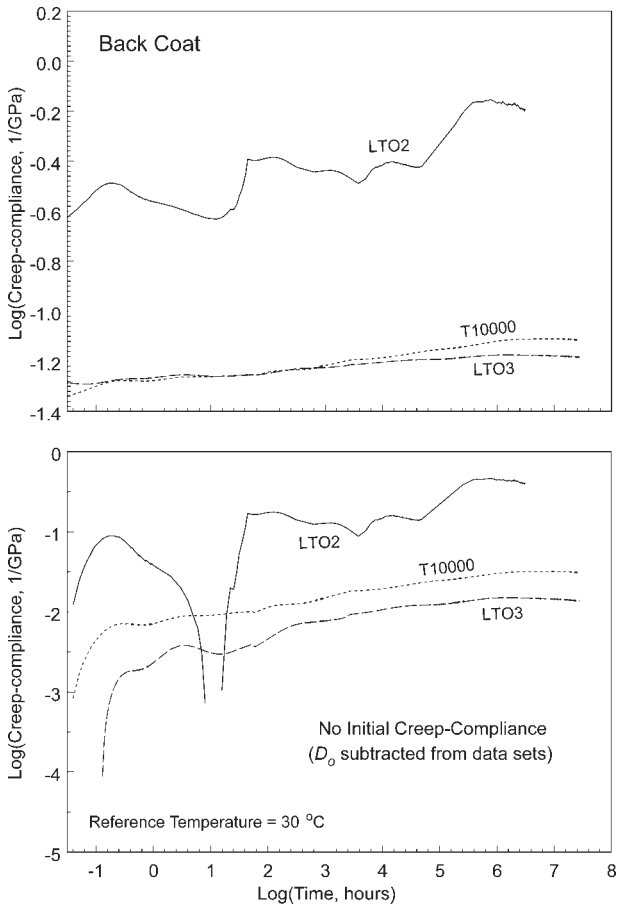

Figure 19 Time-temperature superposition for MP-PEN back coat samples from rule-of-mixtures analysis.

similarities between the substrate back coat and substrate data.

Calculated versus measured results for MP-PEN tapes

To evaluate the validity of the experiments and calculations performed in the rule-of-mixtures approach to separating-out the front coat and back coat compliances, a calculated creep-compliance for the tape can be determined using eq. (6c) and the separate creep-compliances measured for the front coat substrate, substrate, and substrate back coat samples. The calculated creep-compliances for the tape can then be compared with the measured creep-compliances for the tape from separate experiments.

Figure 20 compares the calculated and measured creep-compliances for LTO2, LTO3, and T10000. For LTO2, the calculated versus measured data sets appear to show a close correspondence, with the calculated data set slightly higher. This difference has been attributed to the difficulty in extracting the back coat compliance from the back coat substrate measurements for LTO2.[8] The LTO3 and T10000 calculated data sets appear to be lower than the measured data sets. These differences between calculated and measured data sets could be attributed to errors in initial loading, particularly in the back coat substrate results which could be biased low. Although the back coats appeared to be undamaged from a visual inspection, it was difficult to remove the front coat of the tapes without adversely affecting the back coat. Although the LTO3 and T10000 calculated results are biased low, the shape of the curves is similar to what was observed for the measured data. The slopes are similar out to 10^6 h, and the decrease in compliance for the calculated curves after 10^6 h are similar to what was observed for the measured data.

When the D_o values are subtracted-out in the lower graph of Figure 20, calculated and measured data sets for the MP-PEN tapes collapse onto each other. There are minimal discernable differences between the data sets, although the calculated curve for LTO2 is still slightly higher than the measured

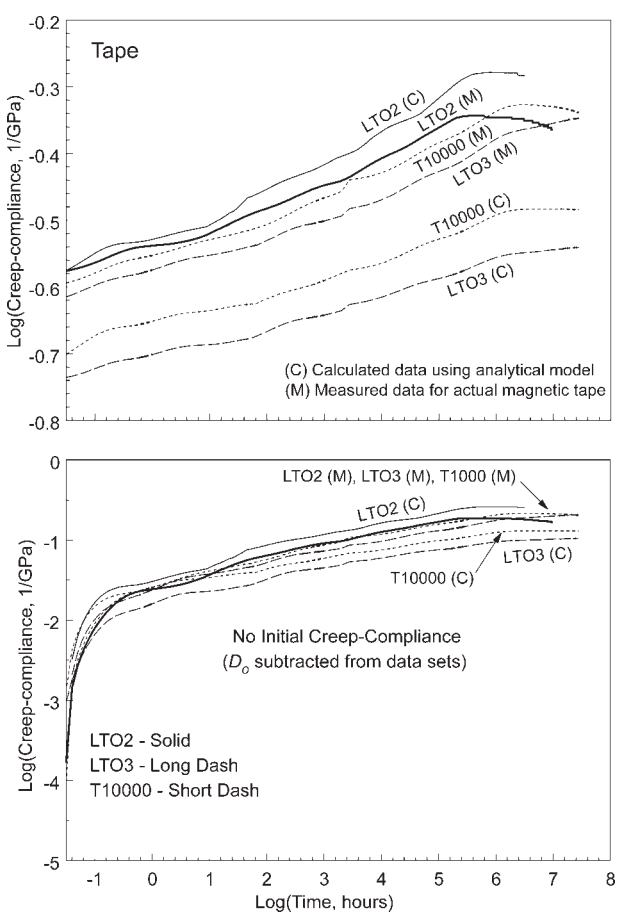

Figure 20 Comparison of calculated and measured creep-compliances for MP-PEN tapes. The calculated data were determined using the rule-of-mixtures model together with experimental results for the substrate. Creep-compliance experiments were performed for the complete MP-PEN tape to determine the experimental data.

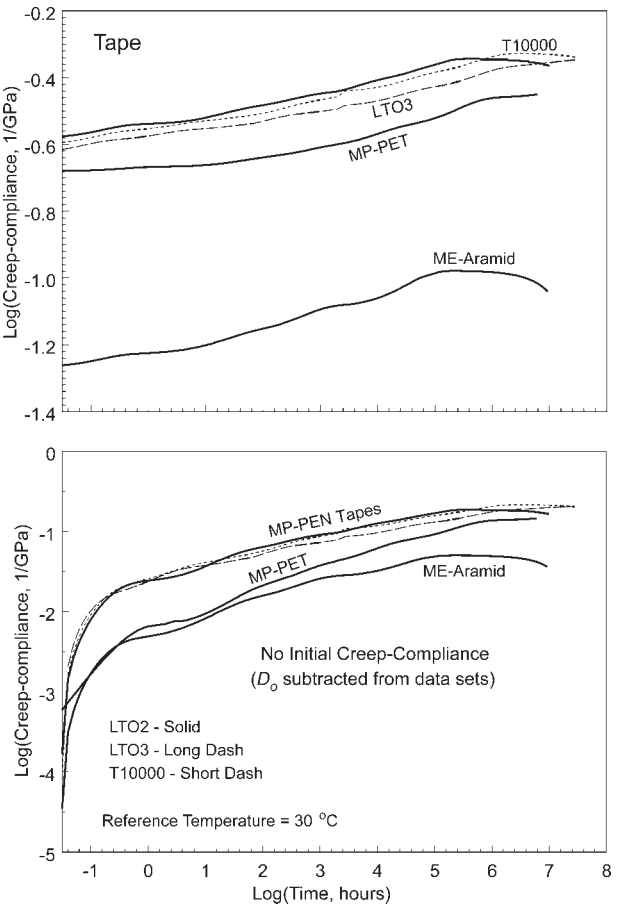

Figure 21 Time-temperature superposition for MP-PEN tapes compared to MP-PET and ME-Aramid tapes.

curve, and the calculated curves for LTO3 and T10000 are slightly lower than their measured curves. Therefore, if the D_o terms are not considered, there is minimal error in the creep-compliance experiments for the dual layer experiments and substrate experiments when compared to the tape experiments. Furthermore, the rule-of-mixtures approach appears to be suitable for making predictions about the creep-compliance behavior of the front coat and back coat.

Comparisons with tapes made from other substrates

Figure 21 shows the creep-compliance curves for the MP-PEN-based tapes (LTO2, LTO3, and T10000) compared to the creep-compliance curves for an MP-PET tape and an ME-Aramid tape. Note that the MP-PET tape has a lower overall creep-compliance than the MP-PEN tapes, and the ME-Aramid tape has a substantially lower creep-compliance. When the D_o values are subtracted-out, the differences in creep-compliance characteristics are still observable. All the tapes experience similar initial increases in creep-compliance, but the rate of creep-compliance appears to slow-down sooner for the ME-Aramid and MP-PET tapes when compared to the MP-PEN tapes. However, after $\sim$ 1 h, all the tapes creep at about the same rate until about 100 h, although the overall compliance for the ME-Aramid and MP-PET tapes is still lower. After $\sim$ 100 h, the MP-PET continues to creep at a higher rate, and the creep-compliance of the ME-Aramid tape diverges from that of the MP-PET and is lower in the longer time periods of 10^6 and 10^7 h. In comparison, the creep-compliance for MP-PET approaches that of the MP-PEN tapes at the end of the experiment.

SUMMARY AND CONCLUSIONS

From the curve fits to determine compliance and viscosity terms, an increasing compliance of the elastomeric binder for the front coat at elevated temperatures could play more of a role in recoverable dimensional changes in the tape. Viscosity terms are negligible at lower temperatures, and correspond with a compliant response to the tape materials. Secondary viscosity terms reach peaks at 30 or 50°C temperatures rather than at 70°C. This appears to be related to more viscous substrate behavior at these lower temperatures. Higher or lower third-term compliance and viscosity terms can be related to some of the subtle changes that occur at higher temperatures or longer time periods.

Creep velocity tends to decrease for PEN-based magnetic tape materials, and this general decrease is due to the characteristics of the PEN substrate. However, characteristics of the front coat due influence the creep characteristics of the tape as a whole, and is indicated by the close correlation between the creep velocities of the front coat substrate and tape samples. Furthermore, at longer time periods, the creep velocity of the front coat substrate samples are higher than the other samples. A reversal in creep velocities occurs at elevated temperatures, and is dominated by the behavior of the PEN substrate. When compared to MP-PET an and ME-Aramid materials, the creep velocity of the MP-PEN materials continues to decrease after longer time periods, where the MP-PET and ME-Aramid materials tend to reach a steady-state creep velocity.

From DMA data for PEN, a β* peak was measured in the E″ data at $\sim$ 50°C, which is before the alpha peak at 160°C. Since the loss modulus corresponds with the viscous behavior of the PEN material, it is interesting to note that the peak in the η_2 viscosity term can also be observed at 50°C from the creep data. Peaks in these parameters correspond with an increase in energy dissipation and nonrecoverable deformation of the PEN polymer. A thorough discussion of the DMA results and literature was provided to understand the characteristics of PEN that are associated with the β* peak.

Amorphous and crystalline regions of PEN appear to be important for dimensional stability, and a higher proportion of *cis* conformation for PEN substrates measured for the LTO4 tape used in this study corresponds with a lower overall loss modulus, which could lead to improved dimensional stability. However, other macroscopic factors such as degree of crystallinity and associated orientation also play a role in dimensional stability.

From the TTS process at a reference temperature of 30°C, similar slopes for the tape samples out to $\sim 10^5$ h indicate similar creep velocity behavior, which can be attributed to substrate behavior. Longer time periods or temperatures higher than 50°C cause a decrease in creep-compliance that could be associated with the β* transition experienced by the substrate. Results for the front coat substrate dual-layer samples indicate that an increase in magnetic particle density could inhibit movement of the binder typically used for MP-PEN tapes. The difference between the creep-compliance behavior of the front coats is clearly observable when the rule-of-mixtures is used to separate-out the compliance characteristics. Since back coat substrate characteristics are similar to that measured for the substrate only, the back coat for MP-PEN tapes is not regarded as having a significant effect on creep for the whole tape.

Creep-compliance results for the MP-PEN-based tapes were also compared with results for MP-PET and ME-Aramid tapes. In general, MP-PET tapes and ME-Aramid tapes have lower overall creep-compliances than MP-PEN tapes. Although initial compliance characteristics are somewhat different, from $\sim$ 1 to 100 h all the tapes creep at approximately the same rate. Longer time periods of $\sim 10^6$ to 10^7 h show that the creep-compliance of MP-PET approaches that measured for MP-PEN.

The author acknowledges the members of the INSIC Tape Program for their support and valuable input throughout the course of the research activity. The author also thanks Ric Bradshaw of IBM for providing the tape, substrate, and dual-layer thickness measurements as well as the dynamic mechanical thermal analysis measurements.

References

1. IBMLTO Ultrium 4 800 GB Data Cartridge, IBM Systems and Technology Group: Somers, New York, 2007.
2. International MagneticTape Storage Roadmap, Information Storage Industry Consortium: San Diego, CA, April 2005.
3. Raymond, R. Alternative Technologies Symposium; Information Storage Industry Consortium: San Diego, CA, 2006.
4. Lee, Y. M.; Wickert, J. A. ASME J Appl Mech 2002, 69, 358.
5. Lee, Y. M.; Wickert, J. A. ASME J Appl Mech 2002, 69, 130.
6. Weick, B. L.; Bhushan, B. J Inf Stor Proc Syst 2000, 2, 1.
7. Weick, B. L.; Bhushan, B. J Appl Polym Sci 2001, 81, 1142.
8. Weick, B. L. J Appl Polym Sci 2006, 102, 1106.
9. Weick, B. L.; Bhushan, B. J Appl Polym Sci 1995, 58, 2381.
10. Press, W. H.; Flannery, B. P.; Teukolsky, S. A.; Vetterling, W. T. Numerical REcipes in C: The Art of Scientific Computing; Cambridge University Press: New York, 1988.
11. Higashioji, T.; Bhushan, B. J Appl Polym Sci 2002, 84, 1477.
12. Aklonis, J. J.; MacKnight, W. J. Introduction to Polymer Viscoelasticity; Wiley: New York, 1983.
13. Canadas, J. C.; Diego, J. A.; Mudarra, M.; Belana, J.; Diaz-Calleja, R.; Sanchis, M. J. Polymer 1999, 40, 1181.
14. Jeong, Y. G.; Jo, W. H.; Lee, S. C. Polymer 2004, 45, 3321.
15. Gillmor, J. R.; Greener, J. Proc Soc Plast Eng ANTEC97 1997, 1582.
16. Tonelli, A. E. Polymer 2002, 43, 637.
17. Hakme, C.; Stevenson, I.; David, L.; Seytre, G.; Boiteux, G. J Non-Cryst Sol 2006, 352, 4746.
18. Berg, J. G.; Wei, T. S.; U.S. Pat. 4,529,645 (1985).
19. Miloslav, N.; Jirat, J.; Kosata, B. Compendium of Chemical Technology (Gold Book), IUPAC: 2006, available at: goldbook.iupac.org/T06406.html.
20. Jones, R. M. Mechanics of Composite Materials, 2nd ed.; Taylor and Francis: Philadelphia, 1999.